Carbohydrate Polymers 88 (2012) 213–222

Contents lists available at SciVerse ScienceDirect

Carbohydrate Polymers

journal homepage: www.elsevier.com/locate/carbpol

Cassava starch–kaolinite composite film. Effect of clay content and clay modification on film properties

J.A. Mbey[a,*], S. Hoppe[b], F. Thomas[a]

[a] Laboratoire Environnement et Minéralurgie, UMR 7569 CNRS-INPL, 15 Avenue du Charmois, B.P. 40, F-54501 Vandoeuvre-Lès-Nancy Cedex, France
[b] Laboratoire Réactions et Génie des Procédés, UPR CNRS 3349, 1 Rue Grandville, B.P. 20451, 54001 Nancy Cedex, France

ARTICLE INFO

Article history:
Received 25 August 2011
Received in revised form
24 November 2011
Accepted 30 November 2011
Available online 9 December 2011

Keywords:
Composite
Kaolinite
Starch
Glass transition
Transparency
Water uptake

ABSTRACT

The influence of kaolinite content within a plasticized starch matrix on the glass transition and decomposition temperatures, water uptake, transparency and UV–vis blocking is reported. Exfoliation of the kaolinite clay within the composite is enhanced when previously intercalated with DMSO. The DMSO-intercalated kaolinite brings in advantages for the clay dispersion within the polymer matrix, the transparency and the water uptake. The transparency of the films is better preserved when DMSO intercalated kaolinite is used and a clay load between 2% and 6%, leads to a significant reduction of the UV light transmission.

1. Introduction

The research in biodegradable polymeric material is of growing interest. There have been extensive studies on natural polymers such as gluten, zein, lignin, cellulose, chitin and starch (Avérous & Halley, 2009). Amongst these, starch is of particular interest. It is a renewable, readily available and a relatively low cost raw material. After appropriate processing, starch as well as other biopolymers, can be used in various applications such as: adhesive, paper, textile, biomedical, thermoset resin, foams and films (Yu, Dean, & Li, 2006). In the domain of packaging application, plasticized starch could help to deal with packaging waste associated with fossil based packaging materials (Sorrentino, Gorrasi, & Vittoria, 2007). However, the water sensitivity, the brittleness and the sensitivity of the mechanical properties to various conditions hinders the expansion of its applications and justifies the constant need for the improvement of starch film properties. The improvement of those properties can be explored in several ways such as blending with other polymers (mostly synthetic) (Parra, Tadini, Ponce, & Lugao, 2004; Pérez, Alvarez, Mondragón, & Vázquez, 2007), cross linking (He, Yaszemski, Yasko, Engel, & Mikos, 2000), composite film preparation (Huang, Yu, & Ma, 2004) and mixed approach that associates blending and composite film preparation (McGlashan & Halley, 2003).

Clays are widely used as fillers in polymer composite materials due to their high aspect ratio and nanometric thickness of their platelets. A good dispersion of small amounts of clay within the polymer matrix gives rise to high surface area for polymer–filler interactions (Ray & Bousmina, 2005). The polymer–filler interactions are also enhanced because of the surface reactivity of the clay that can proceed through hydrogen bonds, complexation, or electrostatic interactions.

For most of the studies on polymer–clay composites, 2:1 clays, such as montmorillonite, laponite and hectorite, are usually used as reinforcing phase, due to their ability to be exfoliated, which results in optimal distribution in the matrix (Avella et al., 2005; Chen & Evans, 2005; Park, Lee, Park, Cho, & Ha, 2003; Park, Misra, Drzal, & Mohanty, 2004; Wilhelm, Sierakowski, Souza, & Wypych, 2003a). Less expandable clays, such as kaolinite, an abundant and ubiquitous 1:1 clay, are rarely used (Carvalho, Curvelo, & Agnelli, 2001; Chen & Evans, 2005; Wilhelm, Sierakowski, Souza, & Wypych, 2003b). To date, many advantages of clay incorporation in starch based material have been demonstrated. Park et al. (2002, 2003) showed that for 5% clay content there was a significant increase of the elongation at break, the tensile strength, the decomposition temperature and a decrease of water vapour diffusion in

* Corresponding author. Tel.: +33 383 596 275; fax: +33 383 596 285.
E-mail addresses: jean-aime.mbey@ensg.inpl-nancy.fr, mbey25@yahoo.fr (J.A. Mbey), Sandrine.hoppe@ensic.inpl-nancy.fr (S. Hoppe), fabien.thomas@ensg.inpl-nancy.fr (F. Thomas).

0144-8617/$ – see front matter © 2011 Elsevier Ltd. All rights reserved.
doi:10.1016/j.carbpol.2011.11.091

potato starch–montmorillonite composite. Wilhelm et al. (2003a) showed that the compression resistance in Cára starch composite is increased by 70% on addition of 50% hectorite but, at the same time, the elongation percentage was reduced of 50%. In 2005, Avella et al., studied the properties of starch–montmonrillonite films and showed, through migration tests, that the films could be satisfactorily used according to the European regulation for biodegradable packaging at date. In all cases, regardless of the type of clay used, its presence within a polymer matrix is shown to significantly influence the polymers properties.

Our interest in this study is the production of composite materials using the abundant and low cost materials: cassava starch and kaolinite clay. For this purpose, the study of physical and chemical properties of the composite material and the understanding of the interactions that determine the observed properties are points of interest. The properties of a polymeric material are determined by the interactions between the polymer chains. In the case of starchy material, flexible films are obtained through the reduction of the chain–chain interactions within raw starch as a result of the addition of a plasticizer. The low energy interaction between the plasticizer and the polymer chains allows an easy sliding of the chains over each other, giving rise to approporiate viscoelastic properties for the use as plastic material. In this work, we use glycerol as the plasticizer because it is an efficient and non toxic plasticizer for starch. Another important element that influences the properties of the composite material is the filler dispersion (Okamoto, 2005). Montmorillonite, which is usually used in polymer–clay composite, is easily dispersed because of the electrostatic repulsion between the clay sheets due to the high electric charge, compared to kaolinite in which the interactions between clay sheets are strong hydrogen bonds. To enhance the dispersion of the kaolinite, within the composite, the intercalation of an aprotic polar molecule such as dimethylsulfoxide (DMSO) within the kaolinite, is an easy way to achieve enough weakening of the clay sheets interactions.

Amongst the most important properties of polymeric materials, the glass transition temperature (T_g), which determines the conditions in which the material can be used and stored (Lourdin, Coignard, Bizot, & Colonna, 1997), is of great interest. Therefore, we focus our interest in assessing the influence of clay content on the T_g of the composite starch film. Another important aspect of polymeric materials is the decomposition behaviour; we also investigate the effect of clay content upon the degradation of the starch matrix. To further investigate the influence of clay content, our interest was also turned towards water uptake (WU) and UV-light barrier properties of the composite film.

2. Materials

2.1. Clay material

A kaolinite-rich clay material was collected in the western region of Cameroon. Its mineral composition is as follows: 76.5% kaolinite; 10.4% illite; 3.4% TiO_2; 2% iron oxide and 4% SiO_2. The kaolin deposit is located at the bottom of a mylonitic cliff. The genesis of this kaolin has been established as a result of a hydrothermal process by Njoya et al. (2006). The sample used in this study is from the sand-poor facies of the deposit that derived from magmatic intrusive veins. The fraction < 40 μm, labelled K3, was collected by means of wet sieving. DMSO intercalated kaolinite (labelled K3D) was prepared using an adapted method from Gardolinski, Carrera, and Wypych (2000). The effectiveness of the intercalation was checked through X-ray diffraction and Fourier transform infra red spectroscopy.

2.2. Cassava starch

The cassava starch was obtained by aqueous extraction from cassava tubers produced in Cameroon. The starch was manually ground and sieved at 100 μm. The sieved starch was stored in a high density polyethylene bottle at ambient temperature. The moisture content, determined by drying to constant weight at 105 °C, is 14%. The ash content determined by ignition of (5 ± 0.1) g of starch at 550 °C in a muffle furnace, is 0.3%. The water binding capacity was 93% (d.b) as determined by a centrifugation method. The elemental CHNS analyser Carlo Erba 1108 was used to determine the following respective contents of carbon, hydrogen and nitrogen: 39.06%, 7.53% and 0.05%. The nitrogen content is very low indicating little protein material.

3. Film preparation

The method of preparation is adapted from Godbillot, Dole, Joly, Roge, and Mathlouthi (2006); Laohakunjit and Noomhorm (2004); and Zeppa, Gouanve, and Espuche (2009). In a 5% aqueous suspension of starch containing 30% (w/w) glycerol with respect to the mass of starch, various amounts of clay (raw or DMSO intercalated) were added. The suspension was then hot mixed at 80 °C during 5 min before being cast and air dried. After drying, the films were stored in low density polyethylene bags under ambient temperature. The amount of kaolinite added is expressed in percentage weight ratio to the mass of starch in the formulation.

4. Characterization

4.1. X-ray analysis

X-ray diffraction patterns were recorded using a D8 Bruker diffractometer with a Co Kα radiation (λ = 1.7890 Å) operating at 35 kV and 45 mA. The diffraction patterns were obtained from 1.5° to 32°(θ) at a scanning rate of 1° min^{-1}. The Bragg law gives access to the basal spacing (d) of the layered silicate: $\lambda = 2d\sin\theta$, where θ is the diffraction angle and λ the wavelength.

4.2. Fourier transform infra red (FTIR) spectroscopy

Infra red spectra were recorded in diffuse reflection mode using a Bruker Fourier Transform Interferometer IFS 55. The spectra, recorded from 4000 cm^{-1} to 600 cm^{-1} with a resolution of 4 cm^{-1}, are obtained by accumulation of 200 scans. The powdered clay or starch (approximately 10 mg) was manually ground with 70 mg of oven dried KBr before analysis.

4.3. Dynamic mechanical thermal analysis (DMTA)

DMTA testing was performed using a Rheometric Scientific DMTA V instrument. Rectangular samples having dimensions 13 mm × 30 mm with an average thickness of 20 μm are used. The imposed deformation was 0.01% at 10 Hz in the temperature range of −100 °C to 90 °C with a heating rate of 5 °C min^{-1}.

4.4. Thermal analysis (DSC)

Differential scanning calorimetry (DSC) was carried out using a Perkin Elmer DSC Pyris 1. A sample of approximately 10 mg is placed in an aluminium pan and sealed. The experience is performed at ambient temperature using ice as cooling source. The samples were heated from 25 °C to 150 °C at a heating rate of 4 °C min^{-1}.

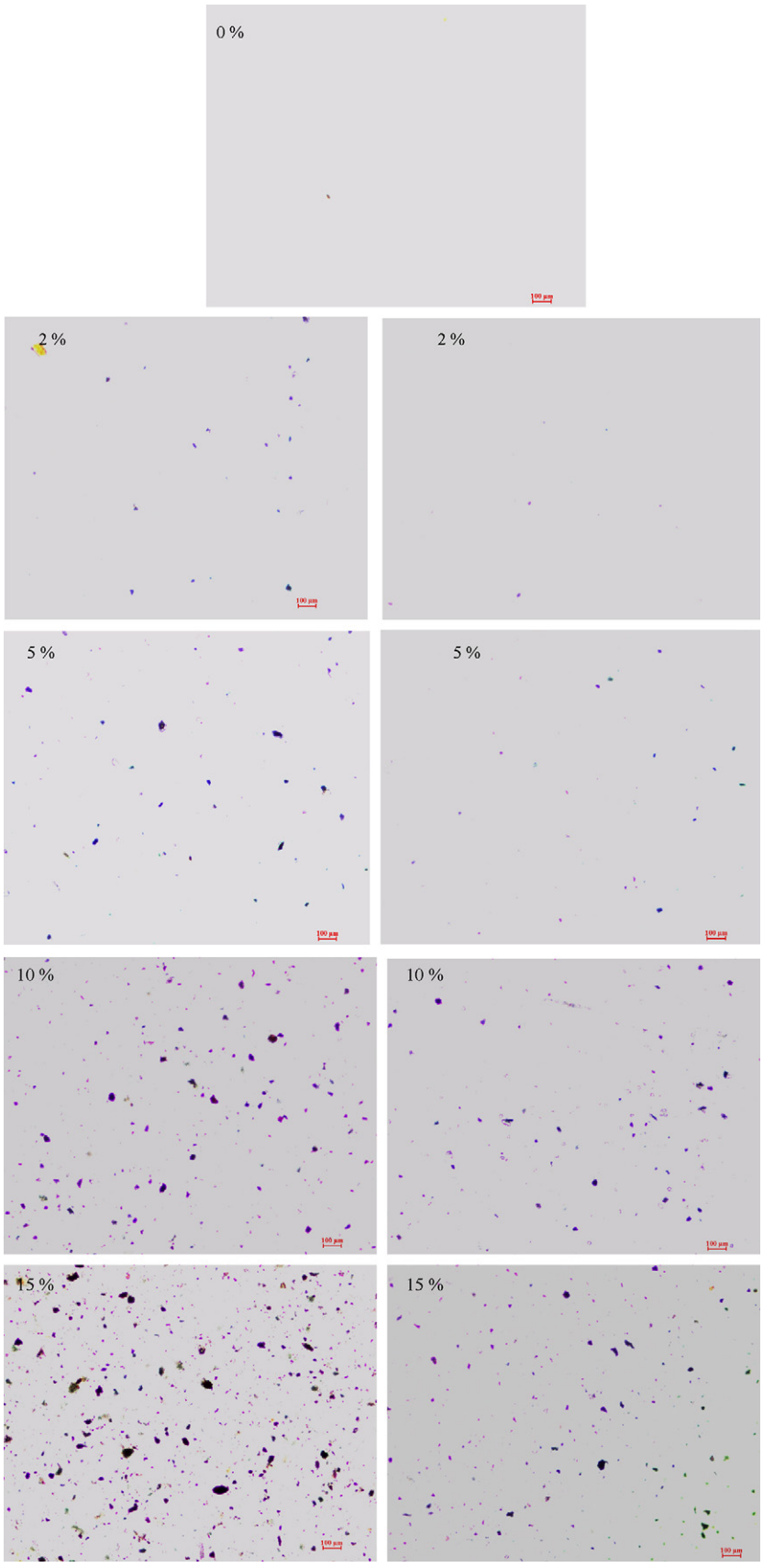

Fig. 1. Optical micrographs of the films with various kaolinite loading. On the left, films loaded with raw kaolinite and on the right films loaded with DMSO intercalated kaolinite.

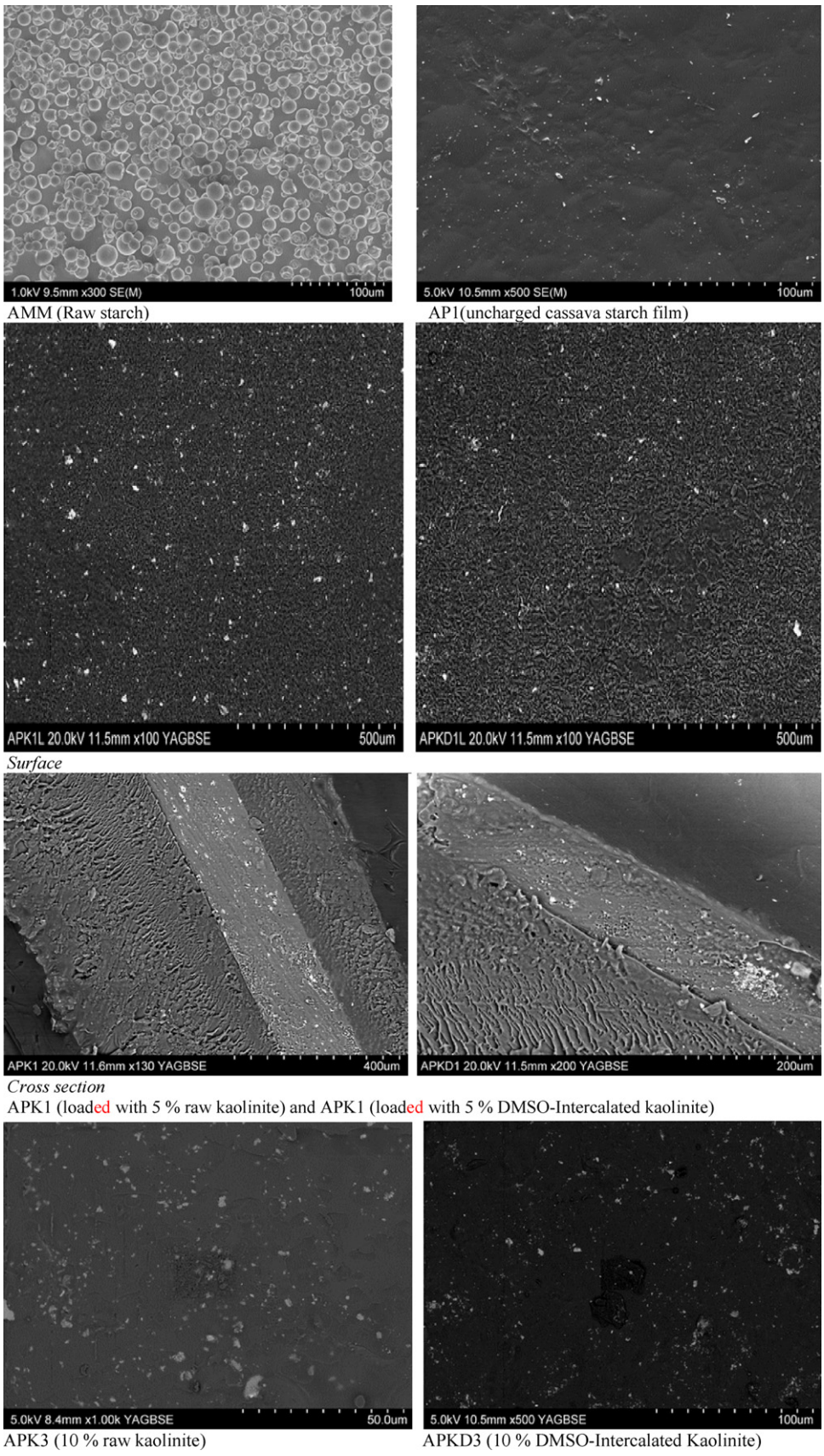

Fig. 2. SEM micrographs of pristine cassava starch film and composites films.

4.5. Optical and scanning electron microscopy (SEM)

The optical observation was done in dark field mode using a Nikon Eclipse LV100 POL microscope. The SEM was achieved on a Hitachi S-4800 using a YAG (Yttrium Aluminium Garnet) backscattered secondary electron detector.

4.6. Water uptake

The water uptake was measured at 100% and 50% relative humidity (RH). For the relative humidity control, we used deionized water (18.2 MΩ cm^{-1}) and 28.15% sodium hydroxide solution in a hermetic container, respectively, for 100% RH and 50% RH. Prior to measurements, pieces of films are oven dried at 60 °C to constant weight (4 h) before being conditioned in the RH atmosphere within the container. At desire time intervals, the films were removed and accurately weighed to ±0.1 mg. The water uptake is calculated as follows:

$$\mathrm{WU} = \frac{m_x - m_o}{m_o}$$

where m_o is the initial mass of the film sample and m_x the mass after equilibrium at a given RH.

The WU was measured after a 24 h because this time it was found to be sufficient for water uptake saturation. The measurements were done in duplicate and the mean values are taken. The maximum deviation for the calculated WU is 0.009.

4.7. Transparency

The transparency of the films was evaluated through UV–vis absorption using a Shimadzu UV 2101 PC. The transmittance spectra of the films are recorded on films with an average thickness of 19 μm.

The blocking effect of the filler to UV transmission was calculated as follows (Sanchez-Garcia, Hilliou, & Lagaron, 2010):

$$\mathrm{Blocking} = \frac{\%T_p - \%T_c}{m_f}$$

where $\%T_p$ and $\%T_c$ refer to percent transmittance, respectively, for the pristine starch film and the composite film; m_f is the percent clay with respect to starch mass.

The blocking effect was calculated for three wavelengths 300 nm, 350 nm and 750 nm, respectively, in UV-B, UV-A and visible region.

5. Results and discussion

5.1. Distribution of kaolinite within the composite

The optical and SEM micrographs are presented in Figs. 1 and 2. From SEM micrographs, it is obvious that the starch granules were completely disrupted during the preparation of the films. Both SEM and optical micrographs show homogeneous surface, which is related to the homogeneity of the films and the quality of clay particles distribution. It is clear from optical micrographs that particles of DMSO treated kaolinite are smaller than those of the raw clay. However, an increase in clay size is observed at loads above 10% which suggests a coagulation of the clay phase. The DMSO–kaolinite is better dispersed within the polymer matrix than the raw material.

5.2. DMSO intercalation

The X-Ray diffraction pattern of raw kaolinite displays the characteristic peak at 7.19 Å (Fig. 3). DMSO treatment results in a complete shift of this peak from 7.19 Å to 11.26 Å, corresponding to a monolayer intercalation of the DMSO molecule in the interlayer space (Olejnik, Aylmore, Posner, & Quirk, 1968). Conversely, the illite phase is not intercalated by the DMSO molecules

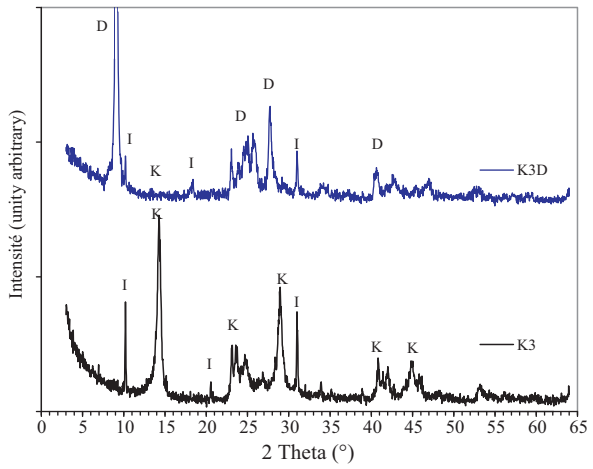

Fig. 3. X-ray patterns of the raw kaolinite (K3) and the DMSO intercalated kaolinite (K3D). I, illite; K, kaolinite; D, kaolinite–DMSO.

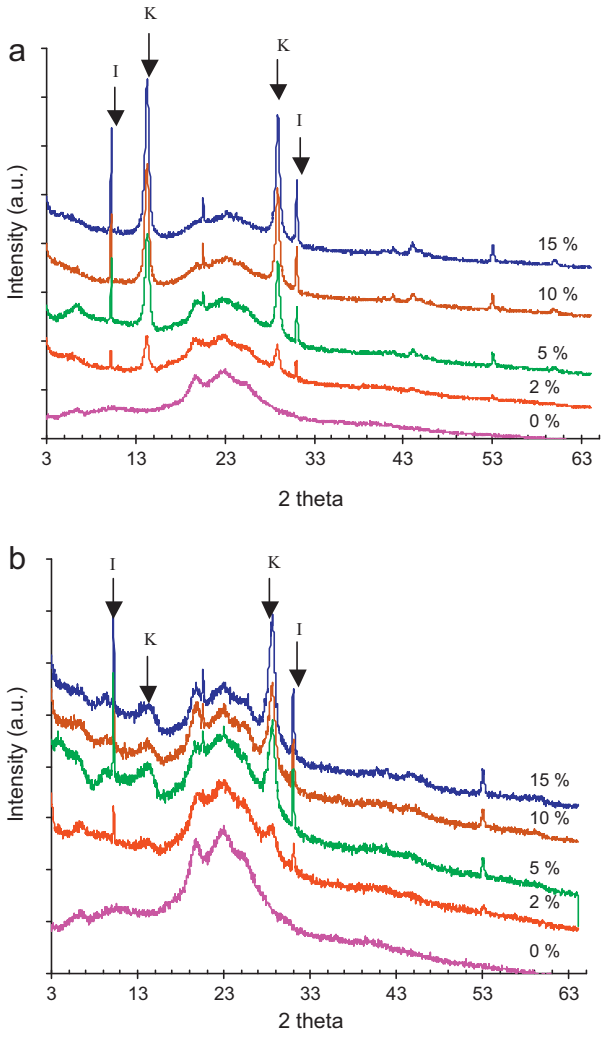

Fig. 4. X-ray patterns of the films at various kaolinite content (a) loaded with raw kaolinite; (b) loaded with DMSO intercalated clay. K, kalinite; I, illite.

as shown by the characteristic peak at 10.07 Å that remains unchanged.

Raw kaolinite incorporated in the starch film still displays the characteristic basal distance at 7.19 Å (Fig. 4a), which indicates that the pseudo-crystals are preserved. However, DMSO intercalated kaolinite is almost completely disordered when incorporated in the starch film, as shown by the absence of both the 7.19 Å and the 11.26 Å peaks (Fig. 4b). This is an indication that the clay dispersion within the starch matrix is more pronounced when DMSO-intercalated kaolinite is used. The use of the Scherrer equation for the calculation of the thickness of the kaolinite coherent domain within the films, from the d_{002} peak (3.58 Å), gives values 203 Å and 120 Å, respectively, in films loaded with raw and intercalated kaolinite, which further confirms the better dispersion of the intercalated kaolinite. The DMSO treatment of the kaolinite leads to almost complete exfoliation of the kaolinite within the composite.

5.3. Clay–starch interactions

In the presence of the raw kaolinite as filler, the bending modes of O—H and C—OH bonds of the starch, respectively, at 995.1 cm^{-1} and 1103.1 cm^{-1} (Fig. 5a and b) are shifted towards higher wavelengths. These shifts are due to clay–starch interactions through hydrogen bonds that are weaker than the chain–chain interactions within the starch. The stretching mode of the carbon skeleton of the starch chains at 2888.8 cm^{-1} is similarly affected (Fig. 5c), which further confirms the weakening of the chain–chain interactions in the starch. These wavelength shifts in films containing the DMSO intercalated kaolinite are larger than those due to the presence of the raw kaolinite, indicating an increase in the kaolinite–starch interactions, due to a better dispersion of the intercalated kaolinite. This observation is in accordance with the X-ray observations.

5.4. Effect of kaolinite on the glass transition temperature of the polymer material

The elastic modulus and the loss tangent evolution of films with various compositions are presented in Fig. 6. The glass transition (T_g) is taken at the maximum of the loss tangent (tan_delta). The loss tangent curves show a secondary transition between −58 °C and −60 °C and this peak was associated to the transition of glycerol rich phase as shown by Famá, Flores, Gerschenson, and Goyanes (2006) and Forssell, Mikkila, Moates, and Parker (1997). The presence of a unique glass transition peak (ranging from 35 to 53 °C amongst all the samples) and the regular evolution of the elastic modulus indicate a good homogeneity of the composite films. Upon clay addition (Fig. 7), the T_g value decreases when the clay content is increased and tends to a limit above 10% of clay.

The addition of DMSO intercalated kaolinite leads to an even lower T_g than for the raw kaolinite. At the glass transition, polymer chains can slide on each other and the T_g lowering indicates that kaolinite facilitates sliding of polymer chains. Hence, because clay addition tends to lower the T_g then this fact constitutes an evidence for plasticizing effect due to the presence of clay. This plasticizing effect is in accordance with the FTIR observations that indicate weakening of starch chain–chain interactions. The lowering of the polymer chain–chain interactions upon clay addition can be attributed first to improvement of starch/glycerol miscibility by the clay/glycerol interactions, and secondly by the polymer chains orientation due to clay presence that help reducing the chain–chain interactions. The modification of the C—H stretching mode in FTIR (Fig. 5) is then associated to the orientation of starch chains and the O—H bending to the increase of starch glycerol miscibility. Regardless of the mode of clay action, because the intercalated clay decreases the T_g more than the raw clay, we conclude that the smaller and better dispersed the clays particles, the better they can play a plasticizing role. This observation associated to X-ray analysis indicates a better dispersion of the DMSO intercalated kaolinite. Because the T_g lowering upon clay addition is limited, we deduce that there is a maximum clay content of interest within the composite.

In addition, at higher clay content, steric effects that favour clay coagulation may appear and lead to coarse particles that, instead of favouring either chain orientation or starch/glycerol miscibility, may hinder them. For the preparation conditions used in this study, the clay content, for maximum influence on the T_g lowering, ranges between 5% and 10% of clay.

5.5. Decomposition temperature

Fig. 8 shows some DSC scans of the cassava starch films (a) and the decomposition temperature evolution as a function of clay loading (b). The glass transition was not detected as is often the case with starch (Róz, Carvalho, Gandini, & Curvelo, 2006).

The decomposition temperature of the starch matrix is moved to higher temperature upon clay loading. This is due to a barrier effect associated to clay that limits the heat diffusion through the starch matrix. The raw kaolinite leads to even higher temperature of decomposition and this was associated to the size of clay particles within the starch matrix. For the intercalated kaolinite, the effect is not very effective between 2% and 5% whereas for the raw kaolinite, the effect is already significant at these loads. Between 5% and 10% of kaolinite, the effect is increased and tends to be stabilized after 10%. It seems as if loading more than 10% of clay does not lead to a greater effect. The weaker effect of the DMSO–kaolinite is in accordance with smaller clay particles as shown by XRD and higher wavelength shifts for O—H and C—OH bending from FTIR. The maximum loading of 10% is correlated by the DMTA analysis and the barrier effect upon starch matrix decomposition appears to be more efficient with the raw kaolinite.

5.6. Water uptake

The water uptake after 24 h (Fig. 9) stay at 50% and 100% relative humidity increases with increasing RH as previously reported (Godbillot et al., 2006; Lourdin et al., 1997; Talja, Yrjo Hélen, Roos, & Jouppila, 2007; Zeppa et al., 2009). Due to the constant glycerol content in all the films, the differences observed are due to clay content and state of dispersion. Therefore, at 100% RH, the films loaded with DMSO intercalated kaolinite exhibit a higher water uptake and this was associated to the dispersion of the clay which generates fine particles giving rise to an increase in polymer chains mobility. This increase in chains mobility indicated relatively weak hydrogen bonds that are disrupted at high RH by water sorption (Talja et al., 2007). The disruption of the hydrogen bonding between the starch and the filler is favoured by the presence of interfaces where water is condensed at high RH. Because the intercalated kaolinite is better dispersed than the raw kaolinite, contribution of clay content to water uptake in films containing intercalated kaolinite is more significant.

At low RH (50%), the clay–polymer interactions are responsible for the limited water absorption observed in the composites films. The use of DMSO–kaolinite leads to higher barrier effects on water uptake due to the fine clay particles present within the starch matrix that enhance the starch–clay interactions and hence, leaving less free hydroxyl groups for water binding. The presence of fine

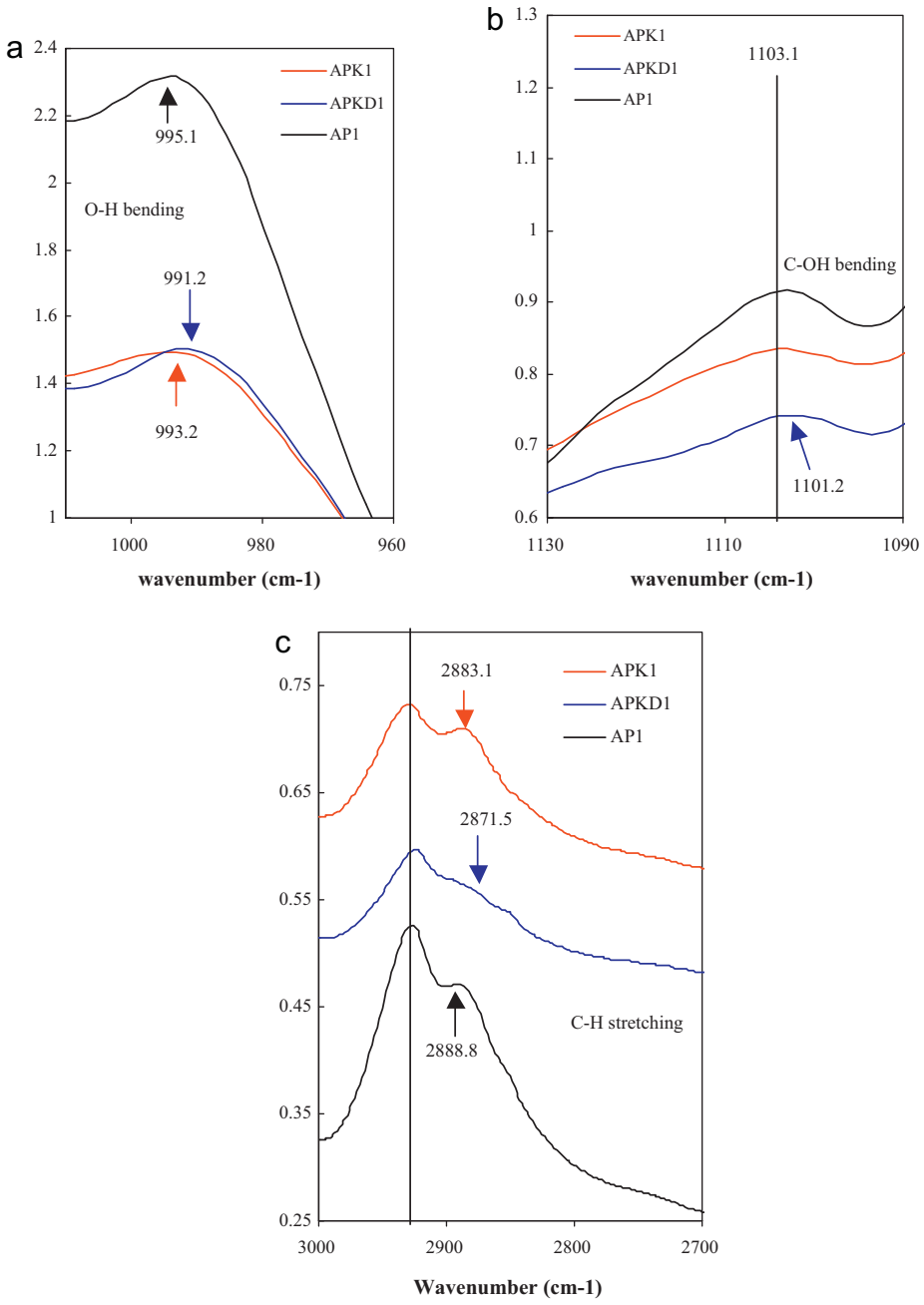

Fig. 5. FTIR bending of (a) O—H; (b) C—OH bonds and (c) stretching of C—H bonds in the composite films. AP1, starch film with 0% kaolinite; APK1, film loaded with 5% raw kaolinite; and APKD1, films loaded with 5% DMSO intercalated kaolinite.

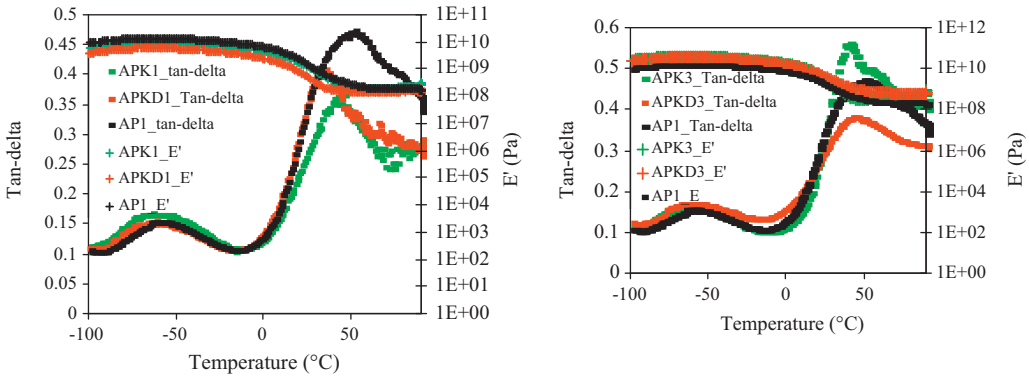

Fig. 6. DMTA analysis: changes in mechanical loss factor (tan-delta) and elastic modulus (E′). AP1 starch film with 0% kaolinite; APK1 and APKD1 films at 5% load, respectively, with raw and DMSO intercalated kaolinite; APK3 and APKD3 films at 10% load, respectively with raw and DMSO intercalated kaolinite.

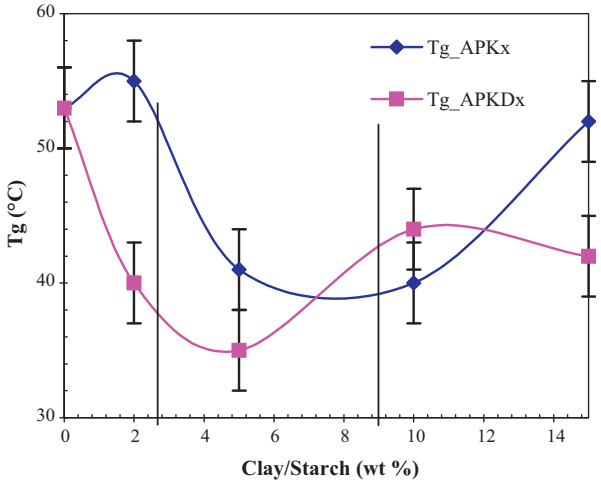

Fig. 7. Variation of glass transition temperature with clay content within the starch matrix. APK*x*, films loaded with raw kaolinite; and APKD*x*, films loaded with DMSO intercalated kaolinite.

clay particles well distributed within the starch matrix also induces a more tortuous path for water diffusion within the polymer matrix.

The water uptake further confirms the better dispersion of DMSO–kaolinite, which enhances the barrier effect to the water uptake.

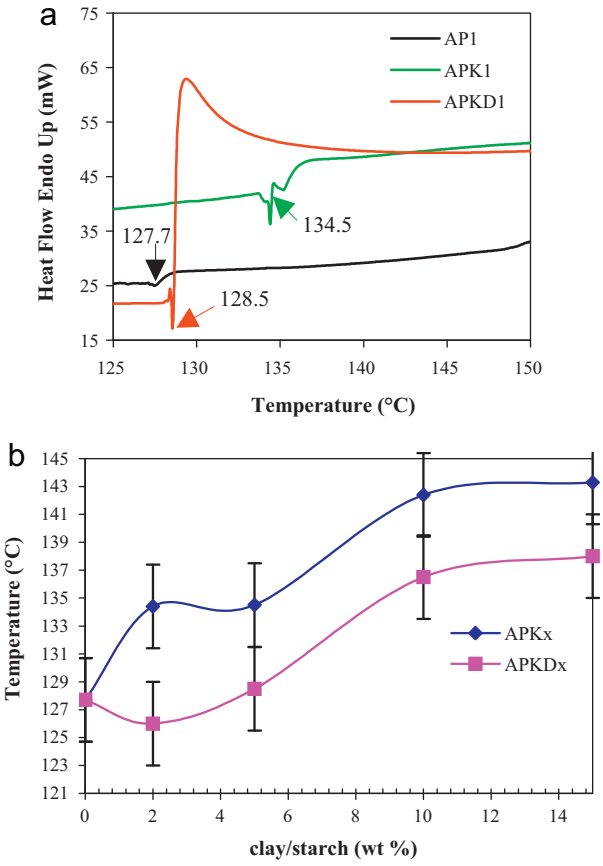

Fig. 8. DSC analysis: (a) DSC scan curves for composites (5% clay load) and neat cassava starch films for decomposition temperature determination; (b) variation of decomposition temperature from DSC as function of clay content. AP1 starch film with 0% kaolinite; APK1 and APKD1 films at 5% load, respectively with raw and DMSO intercalated kaolinite. APK*x*, films loaded with raw kaolinite; and APKD*x*, films loaded with DMSO intercalated kaolinite.

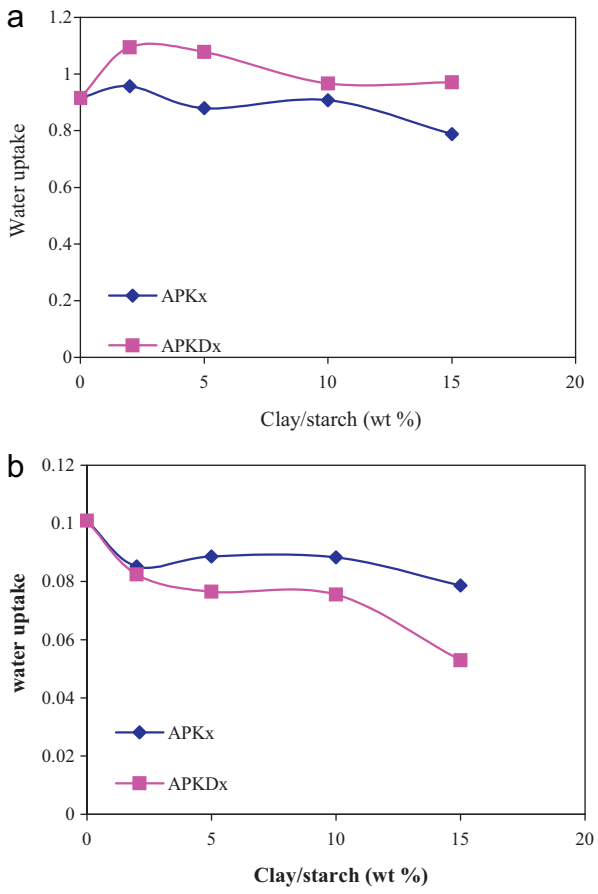

Fig. 9. Water uptake as a function of clay content after 24 h at 100% (a) and 50% (b) RH. APK*x*, films loaded with raw kaolinite; and APKD*x*, films loaded with DMSO intercalated kaolinite.

5.7. Transparency

The transparency of the films was evaluated through transmittance measurements between 300 nm and 800 nm. The aim of this measurement is to further analyse the clay dispersion and to gather information on the blocking effect of clay to UV light. It is well known that the particles larger than the wavelength of visible length would obstruct light. In Fig. 10, we present the visual appearance of the films and in Fig. 11, the UV–vis spectra of the films. The film with 0% clay has the highest transmittance.

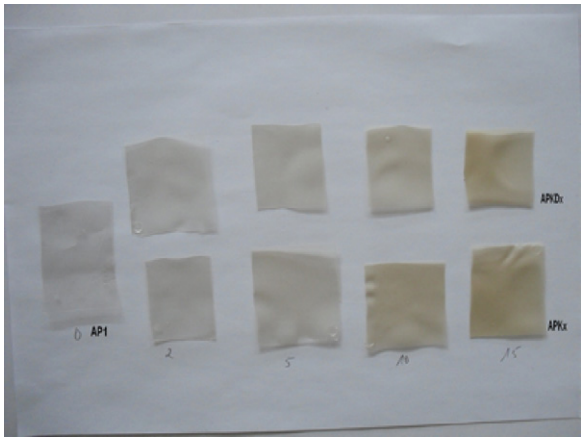

Fig. 10. Films visual appearance.

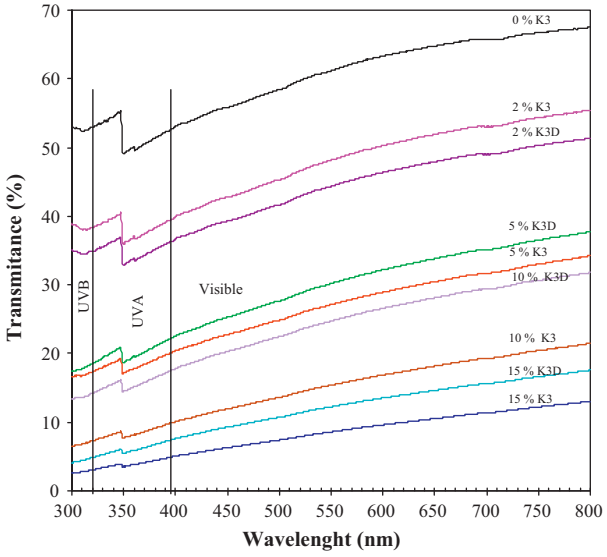

Fig. 11. UV–vis spectra of plasticized cassava starch films at various clay loading. K, kaolinite; raw-K, raw kaolinite; and DMSO-K, DMSO intercalated kaolinite.

When clay is added in the starch matrix, there is a reduction of the transmittance in accordance with the increasing colouring of the samples as observed on the images (Fig. 10). The transmittance of the films loaded with DMSO intercalated kaolinite is higher than that of the films with raw kaolinite and this further proves the better dispersion of the DMSO–kaolinite, which results in smaller size clay particles within the starch matrix. At 2% clay load, there seems to be an inversion because the film loaded with raw kaolinite appears to be slightly more transparent. This fact was associated to the clay distribution within the starch matrix, which may be less efficient at low loading with the raw kaolinite. At low loading, the larger and poorly distributed raw kaolinite particles result in more transparency than the smaller, well-dispersed DMSO–kaolinite particles.

The blocking effect is illustrated in Fig. 12 as a function of clay loading. It appears in Fig. 12 that clay loads ranging from 5% to 10% lead to significant reduction of UV transmission while keeping a significant transparency (Fig. 11). UV-A and UV-B are also reduced upon clay addition but UV-B are less reduced.

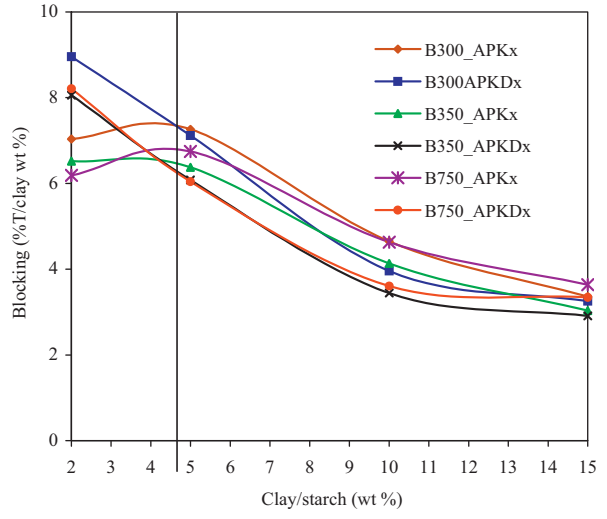

Fig. 12. UV blocking of the films at 300 nm, 350 nm and 750 nm as a function of clay load. APK*x*, films loaded with raw kaolinite; and APKD*x*, films loaded with DMSO intercalated kaolinite.

The use of DMSO intercalated kaolinite is advantageous for transparency conservation and even good UV blocking.

6. Conclusion

In this study, the influence of kaolinite content on properties of composites films made from cassava starch was investigated. The use of DMSO intercalated kaolinite is advantageous for the clay dispersion and distribution, which enhance the effect of clay content on films properties. Dynamic mechanical thermal analysis (DMTA) shows that, the clay content decreases the glass transition temperature (T_g) up to a clay content of 10% with respect to the mass of starch. Clay acts as a plasticizer through a reduction of the interactions between the polymer chains, which promotes their mobility. The use of kaolinite previously intercalated with DMSO results in even lower T_g due to stronger perturbation of the chain–chain interactions. From differential scanning calorimetry (DSC), the degradation temperature of the starch matrix is increased with clay load up to a limit content of 10%.

Furthermore, the water uptake (WU) of the films at 100% and 50% relative humidity (RH) shows that the clay content has an effective barrier effect on WU for low RH but at higher RH, there is an increase of WU in the composites films.

The transparency of the films is less reduced upon addition of the intercalated kaolinite and clay loads between 2% and 6%, lead to significant UV light barrier effect while keeping transparency to a significant extent.

References

Avella, M., De Vlieger, J. J., Errico, M. E., Fischer, S., Vacca, P., & Volpe, M. G. (2005). Biodegradable starch/clay nanocomposite films for food packaging applications. *Food Chemistry*, *93*, 467–474.

Avérous, L., & Halley, P. J. (2009). Plasticized starch based-biocomposites. *Biofuels, Bioproducts and Biorefining*, *3*, 329–343.

Carvalho, A. J. F., Curvelo, A. A. S., & Agnelli, J. A. M. (2001). A first insight on composites of thermoplastic starch and kaolin. *Carbohydrate Polymers*, *45*, 189–194.

Chen, B., & Evans, J. R. G. (2005). Thermoplastic starch–clay nanocomposites and their characteristics. *Carbohydrate Polymers*, *61*, 455–463.

Famá, L., Flores, S. K., Gerschenson, L., & Goyanes, S. (2006). Physical characterization of cassava starch biofilms with special reference to dynamic mechanical properties at low temperatures. *Carbohydrate Polymers*, *66*, 8–15.

Forssell, P. M., Mikkila, J. M., Moates, G. K., & Parker, R. (1997). Phase and glass transitions behaviour of concentrated barley starch–glycerol mixtures, a model for thermoplastic starch. *Carbohydrate Polymers*, *34*, 275–282.

Gardolinski, J. E., Carrera, L. C. M., & Wypych, F. (2000). Layered polymer–kaolinite nanocomposites. *Journal of Materials Science*, *35*, 3113–3119.

Godbillot, L., Dole, P., Joly, C., Roge, B., & Mathlouthi, M. (2006). Analysis of water binding in starch plasticized films. *Food Chemistry*, *96*, 380–386.

He, S., Yaszemski, M. J., Yasko, A. W., Engel, W. P., & Mikos, A. G. (2000). Injectable biodegradable polymer composites based on poly(propylene fumurate) crosslinked with poly(ethylene glycol)-dimethacrylate. *Biomaterials*, *21*, 2389–2394.

Huang, M.-F., Yu, J.-G., & Ma, X.-F. (2004). Studies on the properties of montmorillonite-reinforced thermoplastic starch composites. *Polymers*, *45*, 7017–7023.

Laohakunjit, N., & Noomhorm, A. (2004). Effect of plasticizers on mechanical and barrier properties of rice starch film. *Starch/Stärke*, *56*, 348–356.

Lourdin, D., Coignard, L., Bizot, H., & Colonna, P. (1997). Influence of equilibrium relative humidity and plasticizer concentration on the water content and glass transition of starch materials. *Polymer*, *38*(21), 5401–5406.

McGlashan, S. A., & Halley, P. J. (2003). Preparation and characterization of biodegradable starch-based nanocomposite materials. *Polymer International*, *52*, 1767–1773.

Njoya, A., Nkoumbou, C., Grosbois, C., Njopwouo, D., Njoya, D., Courtin-Nomade, A., et al. (2006). Genesis of Mayouom kaolin deposit (western Cameroon). *Applied Clay Science*, *32*, 125–140.

Okamoto, M. (2005). Biodegradable polymer/layered silicate nanocomposites: A review. In S. Mallapragada, & B. Narasimhan (Eds.), *Handbook of biodegradable polymeric materials and their applications*. American Scientific Publishers, pp. 1–45.

Olejnik, V. S., Aylmore, L. A. G., Posner, A. M., & Quirk, J. P. (1968). Infrared spectra of kaolin mineral–dimethyl sulfoxide complexes. *The Journal of Physical Chemistry*, *72*(1), 241–249.

Park, H., Li, X., Jin, C., Park, C., Cho, W., & Ha, C. (2002). Preparation and properties of biodegradable thermoplastic starch/clay hybrids. *Macromolecular Materials and Engineering*, *287*, 553–558.

Park, H., Lee, W., Park, C., Cho, W., & Ha, C. (2003). Environmentally friendly polymer hybrids. Part 1. Mechanical, thermal and barrier properties of thermoplastic starch/clay nanocomposites. *Journal of Materials Science*, *38*, 909–915.

Park, H., Misra, M., Drzal, L. T., & Mohanty, A. K. (2004). Green nanocomposites from cellulose acetate bioplastic and clay: Effect of eco-friendly triethyl citrate plasticizer. *Biomacromolecules*, *5*, 2281–2288.

Parra, D. F., Tadini, C. C., Ponce, P., & Lugao, A. B. (2004). Mechanical and water vapor transmission in some blends of cassava starch edible films. *Carbohydrate Polymers*, *58*, 475–481.

Pérez, C. J., Alvarez, V. A., Mondragón, I., & Vázquez, A. (2007). Mechanical properties of layered silicate/starch polycaprolactone blend nanocomposites. *Polymer International*, *56*, 686–693.

Ray, S. S., & Bousmina, M. (2005). Biodegradable polymers and their layered silicate nanocomposites: In greening the 21st century materials world. *Progress in Materials Science*, *50*, 962–1079.

Róz, A. L. D., Carvalho, A. J. F., Gandini, A., & Curvelo, A. A. S. (2006). The effect of plasticizers on thermoplastic starch compositions obtained by melt processing. *Carbohydrate Polymers*, *63*, 417–424.

Sanchez-Garcia, M. D., Hilliou, L., & Lagaron, J. M. (2010). Nanobiocomposites of carrageenan, zein, and mica of interest in food packaging and coating applications. *Journal of Agricultural and Food Chemistry*, *58*(11), 6884–6894.

Sorrentino, A., Gorrasi, G., & Vittoria, V. (2007). Potential perspectives of bionanocomposites for food packaging applications. *Trends in Food Science and Technology*, *18*, 84–95.

Talja, R. A., Yrjo Hélen, H., Roos, Y. H., & Jouppila, K. (2007). Effect of various polyols and polyol contents on physical and mechanical properties of potato starch-based films. *Carbohydrate Polymers*, *67*, 288–295.

Wilhelm, H. M., Sierakowski, M. R., Souza, G. P., & Wypych, F. (2003a). Starch films reinforced with mineral clay. *Carbohydrate Polymers*, *52*, 101–110.

Wilhelm, H. M., Sierakowski, M. R., Souza, G. P., & Wypych, F. (2003b). The influenced of layered compounds on the properties of starch/layered compounds composites. *Polymer International*, *52*, 1035–1044.

Yu, L., Dean, K., & Li, L. (2006). Polymer blends and composites from renewable resources. *Progress in Polymer Sciences*, *31*, 576–602.

Zeppa, C., Gouanve, F., & Espuche, E. (2009). Effect of a plasticizer on the structure of biodegradable starch/clay nanocomposites: Thermal, water-sorption and oxygen-barrier properties. *Journal of Applied Polymer Science*, *112*, 2044–2056.